Experimental Investigations of the Flowfield of an Airfoil with Spoiler

Chyang S. Lee*
Stanford University, Stanford, California
and
Satya Bodapati†
Naval Postgraduate School, Monterey, California

An experiment was performed on the flowfields of an airfoil with deflected spoiler at low speed. Surface pressure distributions and boundary-layer and wake profiles were measured systematically to evaluate the effects of angle of attack and spoiler deflection on mean and fluctuating quantities. Boundary-layer and base pressure characteristics were analyzed. The development of wake with angle of attack is hypothesized by the variation of base pressure. The location of hinge bubble depends on boundary-layer characteristics. The wake is self-preserved if a virtual origin is introduced.

Nomenclature

b = wake width
c = airfoil chord
C_C = chordwise force coefficient
C_D = pressure drag coefficient
C_N = normal force coefficient
C_P = surface pressure coefficient
C_{DP} = profile drag coefficient
C_{Pb} = base pressure coefficient
H = boundary-layer shape factor
p = static pressure
p_T = total pressure
u,v = fluctuating velocities in x, y directions
U,V = velocities in x, y directions
U_E = free shear layer or boundary-layer edge velocity
$\overline{uv}$ = Reynolds shear stress
W = wake velocity defect
x_0 = virtual origin
x_t = streamwise position measured from the airfoil trailing edge
α = angle of attack
δ = spoiler deflection angle
δ^* = boundary layer displacement thickness
Γ = vorticity strength

Introduction

A SPOILER is a plate on the upper surface of a wing which can be deflected to spoil the flow and cause separation, thereby decreasing lift and increasing drag. Spoilers are used as effective aerodynamic control surfaces in transport aircrafts. They are usually deflected symmetrically as speed brakes or as lift dumpers at touchdown. When spoilers are deflected asymmetrically, they can provide as much as 90% of the roll control in certain conditions during flight.[1]

The flowfield of an airfoil with spoiler is complex: including separation, reattachment, and vortex shedding. Flow separates from the upper airfoil surface due to the adverse pressure gradient generated by the presence of the spoiler. It reattaches to the spoiler surface at pre-stall angles of attack. A recirculating bubble, called "hinge bubble," is formed upstream of the spoiler hinge. The flow separates again from the spoiler tip and convects into wake as a free shear layer. The flow on the lower airfoil surface also leaves the trailing edge and convects into wake. These separating shear layers form a large bubble downstream of the trailing edge. The shedding vortices from the spoiler tip and the trailing edge make the wake highly turbulent and oscillatory. This unsteady wake affects the effectiveness of spoiler and flap, it may even cause buffet on the control surfaces at the tail of an aircraft. An understanding of the aerodynamics of spoilers is therefore necessary to improve their design.

Experimental investigations of the spoiler problem can be dated back to the 1930's.[2] Most of the early works were confined to steady parameters, such as static surface pressure, lift, drag, and moment. Complete flowfield measurements, including boundary-layer development and associated wake characteristics, were conducted at Wichita State University.[3-5] A series of experiments were also initiated by the Joint Institute for Aeronautics and Acoustics of Stanford University and the Aerodynamics Research Group of Boeing Airplane Company.[6] The measurements included flow visualization, steady and unsteady surface pressures, and mean velocities of the flowfield. The mean and unsteady surface pressures were reported by McLachlan et al.[7] and Ayoub et al.[8]; the boundary-layer and wake profiles were reported by Lee et al.[9] These investigations illustrated the basic flowfield structure, but the influence of geometrical conditions (e.g., angle of attack and spoiler deflection) is still not clear.

In the present experimental study, the mean and fluctuating quantities on the airfoil surface and in the wake were measured systematically at different angles of attack and spoiler deflections. Parallel to the experimental investigations, a computational analysis based on simple vortex tracing methods was also initiated.[10] The objective of this experiment is to investigate the effect of geometrical conditions, and to provide a complete experimental data base to be compared with the computational results.

Received July 22, 1986; revision received Feb. 16, 1987.

*Postdoctoral Fellow, Joint Institute for Aeronautics and Acoustics, Department of Aeronautics and Astronautics. Member AIAA.

†Associate Director, Navy-NASA Joint Institute of Aeronautics, Department of Aeronautics. Member AIAA.

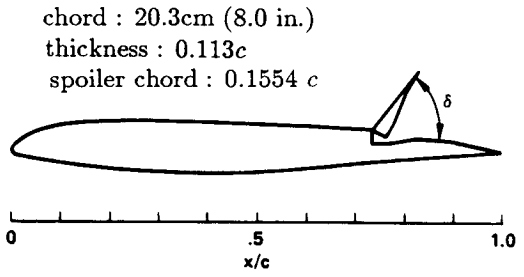

Fig. 1 Airfoil cross section.

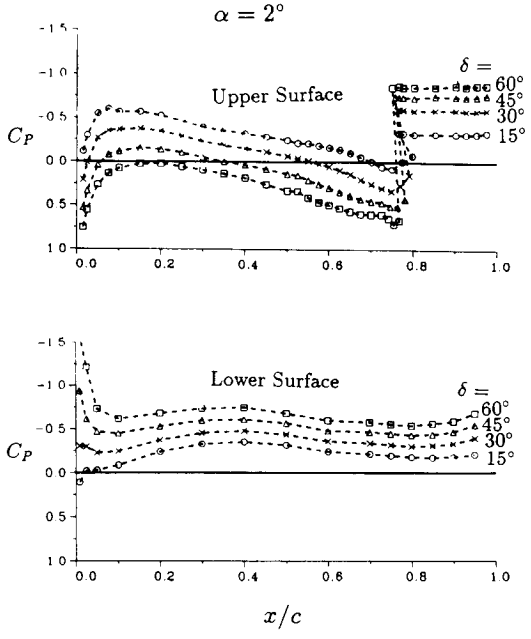

Fig. 2 Typical surface pressure distributions.

Experimental Setup and Measurements

The experiment was conducted in the Stanford low-speed closed-circuit wind tunnel having a 45.7 × 45.7-cm (18 × 18 in.) test section. A traversing mechanism fitted to the test section provides the support for sensors. Stepper motors drive the sensor support along three axis. The minimum step size is 0.0127 mm (0.0005 in.), which is capable of resolving the detailed profiles of boundary layers and wake. The experiment was fully integrated with a minicomputer for on-line data acquisition and analysis.

The basic airfoil model is a Boeing advanced transport research airfoil with 20.3-cm (8-in.) chord and maximum thickness ratio of 11.3% as shown in Fig. 1. A spoiler of 15.5% chord length is hinged at 73% chord. Boundary-layer trips made of 0.254-mm (0.01-in.) diam glass balls were placed from the leading edge to 7.5% chord on both sides of the airfoil. The freestream velocity was maintained at a nominal value of 20 m/s, corresponding to a Reynolds number of 2.8×10^5 based on the chord. This airfoil section was selected because of the availability of some experimental data from larger wind tunnels[4] for a comparison on scale effects.

The mean surface pressure distribution was measured through 84 static pressure taps distributed over the airfoil. Total and static pressures in the wake were measured by a standard pitot-static tube. Single hot wires were used for boundary-layer measurements. Wake measurements were conducted by both single wires and cross wires to obtain mean velocities and turbulent stresses.

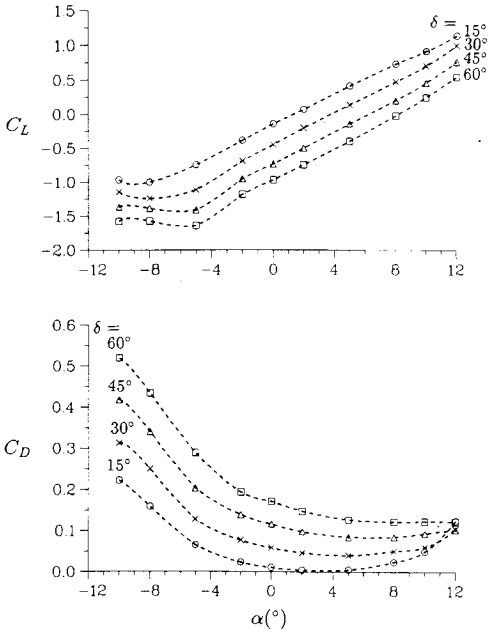

Fig. 3 Variation of lift and drag coefficients with angle of attack.

Discussion of Results

Experiment was carried out over a range of spoiler deflections (0, 15, 30, and 60 deg) and angles of attack (from −10 to 12 deg). The details can be found in Ref. 11; only typical results are presented here.

Mean Surface Pressure

Mean pressure distributions are shown in Fig. 2. In this figure, α is kept at 2 deg and δ is varied from 15 to 60 deg to examine the effect of spoiler deflection. The suction on the upper surface upstream of the spoiler and the pressure on the lower surface of the airfoil decrease with δ, but the constant suction downstream of the spoiler (base pressure) increases with δ. However, the gain in the base pressure region is less than the loss of suction upstream of the spoiler on upper surface, therefore, total lift still decreases with δ. The effect of α and δ on lift is illustrated more clearly by plotting C_L against α for different δ as shown in Fig. 3. At a fixed spoiler deflection, lift increases with angle of attack. The average slope of the lift curve is 5.90/rad, which is near the theoretical value of 2π for a nonseparated thin airfoil. Lift reaches a minimum when α is less than −5 deg for $\delta = 45$ deg and 60 deg, this can be attributed to the early separation on the lower surface of the airfoil and will be discussed in the analysis of the base pressure.

Figure 3 also shows pressure drag C_D as a function of α and δ. At a fixed angle of attack, C_D increases with δ as expected, but the drag curves have two different slopes. For example, at a fixed spoiler deflection of 60 deg: $dC_D/d\alpha \approx 0$ for 2 deg < α < 12 deg, and $dC_D/d\alpha \approx -2.3$ for −10 deg < α < −2 deg. This nonlinear behavior can be explained as follows: When $\alpha < 0$ deg, the frontal projection area of the model increases with the negative angle of attack, thereby increasing C_D. At positive angles of attack, the normal force coefficient C_N increases with α while the chordwise coefficient C_C decreases with α due to the suction near the leading edge. The pressure drag is obtained by

$$C_D = C_N \sin\alpha + C_C \cos\alpha \qquad (1)$$

the contribution from $C_C \cos\alpha$ offsets the increase in $C_N \sin\alpha$, therefore C_D is not changed.

Fage and Johansen[12] correlated the base pressure C_{Pb} and the vorticity flux $d\Gamma/dt$ on a number of bluff body flows as

$$C_{Pb} = 1 - U_E^2/U_\infty^2$$
$$\frac{d\Gamma}{dt} = \frac{1}{2} U_E^2 \tag{2}$$

where U_E is the velocity on the outer edges of the free shear layer. This correlation shows that base pressure is determined by the strength of vorticity flux; for example, a strong vorticity flux produces larger wake edge velocity U_E resulting in a lower base pressure.

Figure 4 shows the variation of C_{Pb} with α for different δ. There are four regions of C_{Pb}. For $\delta = 60$ deg, C_{Pb} remains almost constant in region III, indicating that the basic structure of the flowfield does not change with α. However, C_{Pb} increases with α in regions I and IV, whereas it decreases in region II. A probable development of the flowfield is illustrated in Fig. 5.

1) For moderate angles of attack (0 deg $< \alpha <$ 8 deg), a hinge bubble is formed ahead of the spoiler (Fig. 5a). Flow separates from the spoiler tip and generates a strong vorticity flux whose strength is insensitive to α. Hence, C_{Pb} holds constant.

2) For higher angles of attack ($\alpha > 8$ deg), flow on the airfoil upper surface separates well ahead of the spoiler hinge line (Fig. 5b). The spoiler is immersed inside the separated region with low velocities. The vorticity flux shed from the spoiler tip becomes weaker thereby increasing C_{Pb}.

3) For moderate negative angles of attack (-5 deg $< \alpha < 0$ deg), the hinge bubble is washed away by the incoming flow (Fig. 5c). Separation on the upper surface occurs at the spoiler tip only. A rather weak vorticity flux is induced at the spoiler tip by the weak vorticity flux at the trailing edge, consequently, C_{Pb} increases.

4) As the angle of attack decreases further ($\alpha < -5$ deg), flow on the lower surface separates upstream of the trailing edge (Fig. 5d). The trailing edge vorticity flux is weak since it is inside the "dead water" region of the wake from the airfoil lower surface. However, vorticity flux from the spoiler tip is stronger because a larger U_E at the spoiler tip is induced by the two vorticity flux shed on the lower airfoil surface, hence C_{Pb} decreases in this region.

Figure 6 compares the surface pressure distribution of the present measurements and the data from a larger wind tunnel at Wichita State University[4] ($Re = 2.2 \times 10^6$). The agreement is reasonable on the lower surface. The discrepancy on the upper surface near the leading edge can be attributed to the boundary-layer trip used in the present experiment. The difference in the hinge bubble region and the base pressure is believed due to the scale effect on the upper surface boundary layer, this is discussed in the following section.

Boundary Layer

Typical mean and rms boundary layer profiles on the upper surface of the airfoil are presented in Figs. 7 and 8. Laminar boundary layers can be observed at $\alpha = 0$ deg. As α increases to 5 deg, the boundary layers become turbulent. The boundary-layer trip apparently did not trigger the transition at low angles of attack. An explanation is given as follows: Comparing the pressure distribution on the upper surface for $\delta = 60$ deg at two angles of attack, 2 and 8 deg, as shown in Figs. 2 and 6, the suction peak near the leading edge for $\alpha = 8$ deg is higher than the case of $\alpha = 2$ deg, while the pressure in the hinge bubble region is about the same. The corresponding adverse pressure gradient at high angles of attack is therefore much larger than that at low angles of attack. Decelerated flows are more likely to become unstable, hence the boundary layer is easier to be triggered at higher angles of attack.

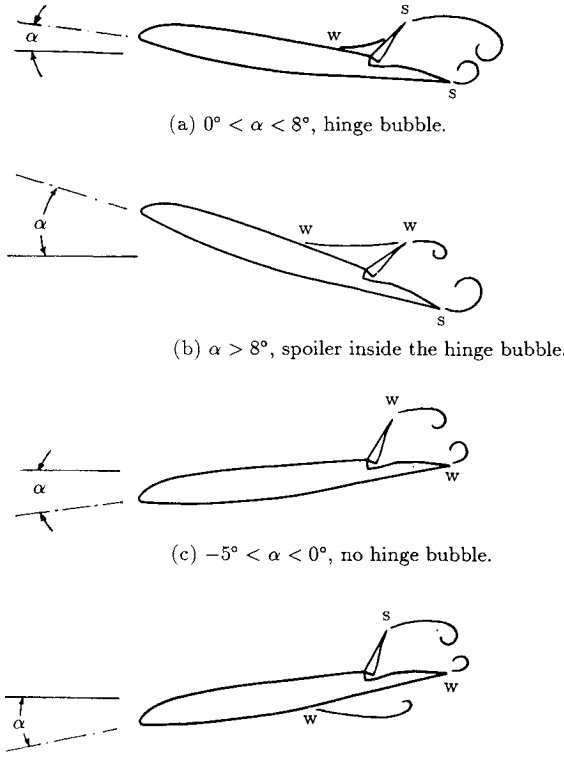

Fig. 5 Development of near wake at different ranges of angle of attack.

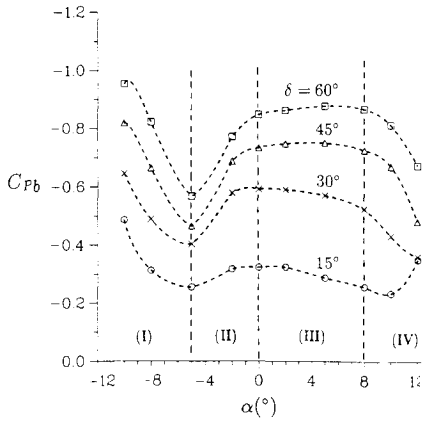

Fig. 4 Variation of base pressure coefficient.

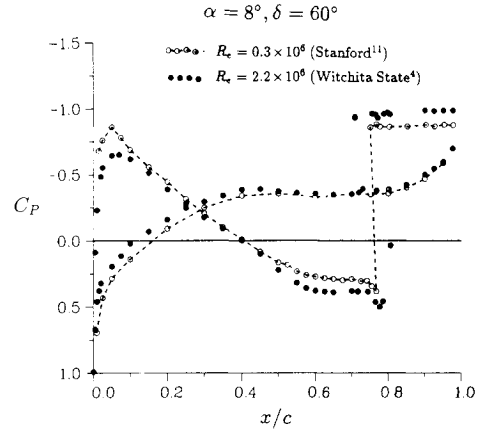

Fig. 6 Scale effect on the surface pressure measurements.

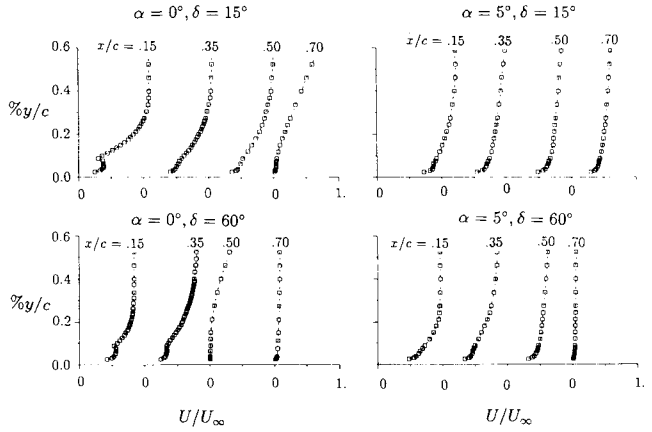

Fig. 7 Boundary-layer mean velocity profiles.

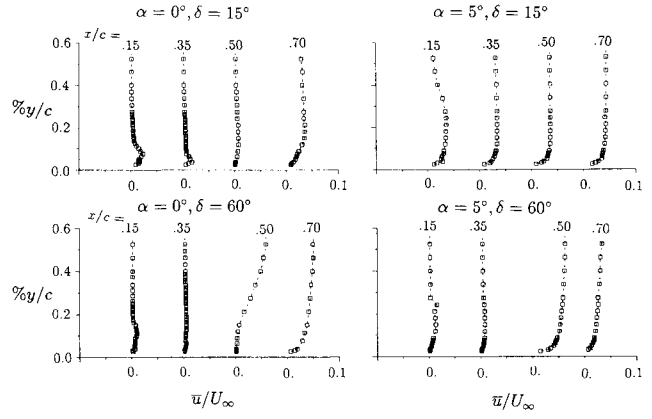

Fig. 8 Boundary-layer rms velocity profiles.

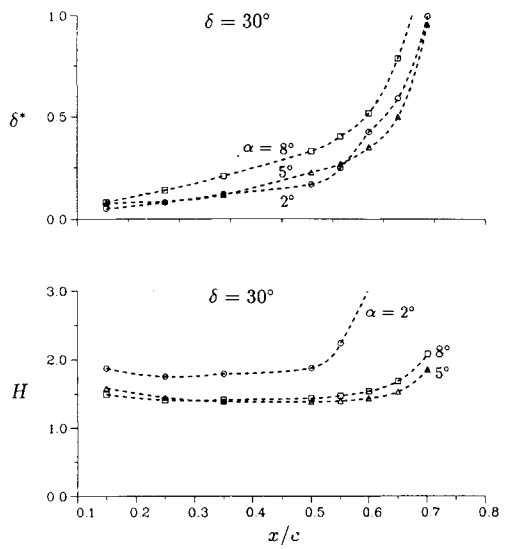

Fig. 9 Development of δ* and H on the airfoil upper surface.

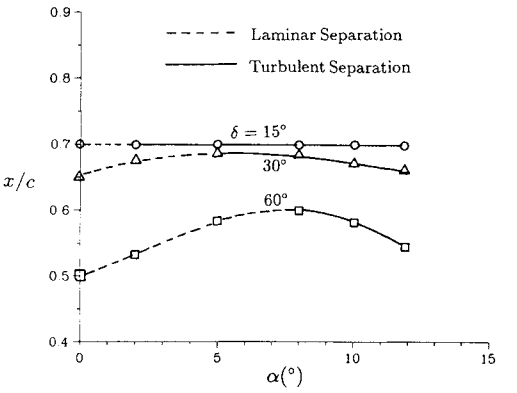

Fig. 10 Location of the hinge bubble separation.

Separation of laminar boundary layers can be detected from the vanishing wall shear stress, i.e., $(dU/dy)_W = 0$. For example, a laminar hinge bubble separation occurs at $x/c = 0.70$ for $\alpha = 0$ deg, $\delta = 15$ deg, and moves upstream to $x/c = 0.50$ as δ increases to 60 deg while maintaining α at 0 deg. This agrees with the rapid increase of the rms velocities at the corresponding locations. An S shape can be observed close to the surface near the leading edge on the mean velocity profiles at $x/c = 0.15$ for $\alpha = 0$ deg, $\delta = 15$ deg, and at $x/c = 0.15$ and 0.35 for $\alpha = 0$ deg, $\delta = 60$ deg. This is believed to be a laminar leading edge separation. Since the hot wire cannot determine the direction of the flow, the lower part of the S profiles is the reverse flow but plotted in the positive direction. For $\alpha = 0$ deg, $\delta = 15$ deg, this S shape disappears at $x/c = 0.35$, indicating the flow reattaches to the surface. For $\alpha = 0$ deg, $\delta = 60$ deg, a long leading edge bubble which extends to $x/c = 0.35$ can be observed. The formation of the laminar leading edge bubble results from the adverse pressure gradient downstream of the minimum pressure peak. The laminar leading edge bubble is very unstable and sometimes becomes turbulent a short distance downstream of the separation. In the present experiment, the boundary layer remains laminar until it separates further downstream into the hinge bubble.

No laminar leading edge bubble can be observed as the angle of attack increases to 5 deg or higher. The wall shear stress increases with α indicating that the boundary layer becomes turbulent. The turbulent boundary layer can also be observed by thickening of the rms profiles in Fig. 8. For the separation of turbulent boundary layers, there is no sharp change on the mean and rms profiles. To locate the turbulent separation point, the variation of displacement thickness δ^* and shape factor H along the chord are plotted in Fig. 9. An abrupt increase of δ^* is an indication of the onset of separation. The turbulent separation point can be approximated by H reaching a value between 1.8 and 2.4.[13]

The effect of angle of attack and spoiler angle on the type of boundary layers and the location of the hinge bubble separation is shown in Fig. 10. The extent of laminar boundary layer is larger for higher spoiler angle. At a fixed spoiler angle, separation point moves downstream with angles of attack. This is due to the transition of boundary layers, since the turbulent boundary layer is more energetic and can resist higher adverse pressure gradient.

In the potential theory, the surface pressure coefficient C_P is related to the local boundary layer edge velocity U_E by

$$C_P = 1 - (U_E/U_\infty)^2 \tag{3}$$

A comparison of U_E between the direct hot-wire measurement and the derived values from C_P is shown in Fig. 11. The agreement is reasonable even in the separated hinge bubble region. The figure shows that as long as U_E is taken as the edge velocity on the separated shear layer, Eq. (3) holds for the attached flow as well as the separated region. These results support the assumption in the free vortex sheet method,[14] which approximates a stalled airfoil by using the free vortex sheets in the separating boundary layer region and solving the associated potential flow problem to obtain the surface pressure distributions.

Wake

The profile drag can be evaluated from the measured total and static pressures in the wake by the following relation[15]:

$$C_{DP} = 2\int \left(\sqrt{\frac{p_T - p}{p_{T\infty} - p_\infty}} - \frac{p_T - p}{p_{T\infty} - p_\infty} \right) d\left(\frac{y}{c}\right) \qquad (4)$$

The variation of C_{DP} with x_t/c at $\alpha = 0$ deg is plotted in Fig. 12 for different spoiler deflections. The profile drag always starts at the maximum and decreases asymptotically downstream. This variation is due to oscillations of the free shear layers. Equation (4) is derived for steady flows, and the turbulent stresses are neglected in the momentum equation. Therefore, the loss of momentum flux (profile drag) is overestimated in the near wake. The profile drag coefficient should be more reliable in the downstream locations because the fluctuating velocities decay along the wake.

The pressure drag coefficient C_D obtained by integrating the surface pressures around the model is also plotted in Fig. 12. The drag due to skin friction is not included in the pressure drag so the profile drag coefficient C_{DP} should always be larger than the pressure drag coefficient C_D. However, C_{DP} is less than C_D at $x_t/c = 1.5$ for $\alpha = 0$ deg, $\delta = 60$ deg. This is opposite to the trends shown in other cases. This deviation can be attributed to the wind tunnel wall effect in the wake. Although all the cases should suffer from the blockage effect, this discrepancy is observed only at $\delta = 60$ deg where the wake blockage is largest in the test cases.

The wake profiles and turbulent stresses measured by cross hot wires are presented in Fig. 13 for $\alpha = 0$ deg, $\delta = 60$ deg at three stations. The longitudinal velocity profiles are compared with the pitot tube data. The agreement is reasonable except at $x_t/c = 0.25$. Probes are inside the reverse flow region at this location. Hot wires rectify the reverse flow and show larger velocities. Pitot tube cannot measure the negative velocity either, but the fluctuation is damped by the air inside the tube, so the pitot tube results show a larger velocity defect. Both measurements are in error at $x_t/c = 0.25$, but the pitot tube profile should be more realistic than the hot-wire result. The longitudinal turbulent stresses show two peaks at the locations corresponding to the two free shear layers shed from the spoiler tip and the airfoil trailing edge. The S shape in the transverse velocity and Reynolds shear stress are typical for a two-dimensional wake.

The wake width and velocity defect can be deduced from the velocity profiles. The wake width b is defined by the distance between two points where the velocity defect W is one half of the maximum velocity defect W_0. Assuming a two-dimensional self-preserved wake, b and W_0 can be correlated with the streamwise location x_t by

$$\frac{b}{c} = k_b \sqrt{\frac{x_t + x_0}{c}} \qquad \frac{W_0}{U_\infty} = k_w \sqrt{\frac{c}{x_t + x_0}} \qquad (5)$$

where x_0 is the "virtual origin" of the wake. The growth of b and W_0 in the streamwise direction is plotted in Figs. 14 and

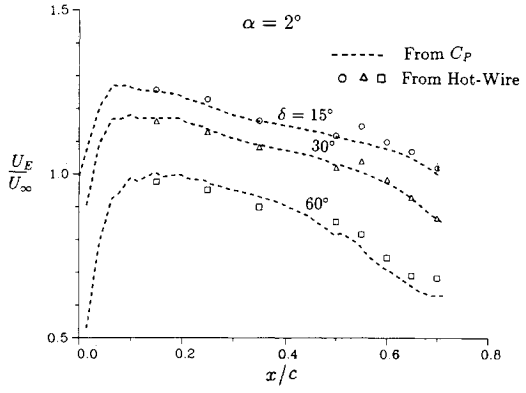

Fig. 11 Comparison of U_E from hot-wire and surface pressure measurements.

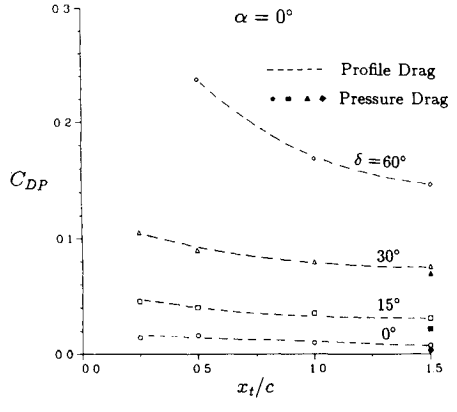

Fig. 12 Variation of profile drag downstream of the airfoil trailing edge.

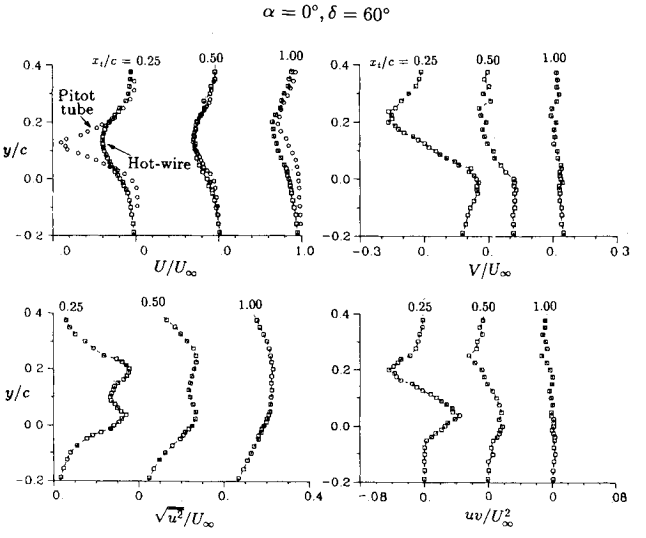

Fig. 13 Velocity and turbulent stress profiles in the wake.

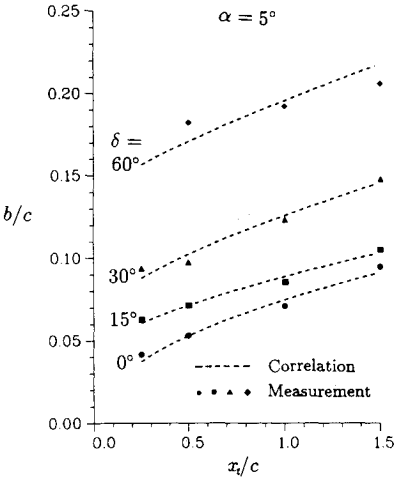

Fig. 14 Correlation of wake width with the streamwise location.

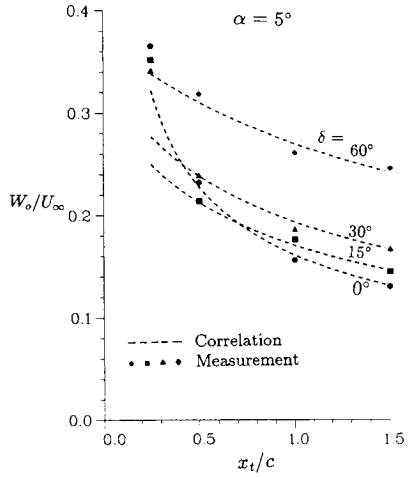

Fig. 15 Correlation of maximum velocity defect with the streamwise location.

Table 1 Correlation constants of self-similar wakes, α = 5 deg

δ	0 deg	15 deg	30 deg	60 deg
x_0	0.016	0.403	0.463	1.073
k_b	0.0746	0.0749	0.104	0.136
k_w	0.161	0.232	0.234	0.389

15 for $\alpha = 5$ deg and four spoiler deflections. The wake width and the maximum velocity defect reasonably agree with the correlation except at $x_t/c = 0.25$. This deviation can be attributed to large fluctuation of velocities in the near wake. The correlated values of x_0, k_b, and k_w are listed in Table 1. The virtual origin is equal to 0.016 for $\delta = 0$ deg, which is in the same range of $x_0/c = 0.025$ obtained by Spence[16] for a nonseparated flow. Compared with the nonseparated flows, the virtual origin is located much upstream for $\delta = 15$ deg and 30 deg (0.403 and 0.463% chord). The value of x_0/c for $\delta = 60$ deg is not considered to be reliable because of the measurement error and wind-tunnel wall interference mentioned earlier.

The surface pressure distributions, mean velocity profiles and turbulent stresses in the wake, and the wind-tunnel wall effects were calculated by the vortex tracing method. Good agreement was found in comparing the calculated results and the present measurements. The detailed description of the numerical methods and the comparison can be found in Ref. 10.

Conclusions

1) Base pressure behind the spoiler changes rapidly with angle of attack. The development of wake at different angles of attack is hypothesized by the variation of base pressure.

2) The location of hinge bubble depends on the boundary layer characteristics. At low angles of attack and large spoiler deflections, a laminar hinge bubble can extend up to 25% of the chord. At high angles of attack, the boundary layer becomes turbulent and the hinge bubble is smaller.

3) Profile drag calculated by integrating the pressures in the near wake may not be reliable for an unsteady wake with massive separation, the turbulent stresses cannot be neglected in the calculation.

4) The wake is self-preserved if a virtual origin is introduced. The virtual origin is located near the mid-chord for $\delta = 15$ and 30 deg, which is farther upstream than a nonseparated flow.

Acknowledgments

This work is supported by the Aerodynamics Research Group of Boeing Airplane Company, monitored by Mr. M.D. Mack and Dr. H.C. Seetharam. The authors are grateful for their cooperation and useful discussions during the course of this work.

References

[1]Mack, M.D., Seetharam, H.C., Kuhn, W.J., and Bright, P.T., "Aerodynamics of Spoiler Control Devices," AIAA Paper 79-1873, 1979.

[2]Weick, F.E. and Short, J.A., "Wind Tunnel Research Comparing Lateral Control Devices, Particularly at High Angles of Attack—Spoiler and Ailerons on Rectangular Wings," NACA Rept. 439, 1932.

[3]Seetharam, H.C. and Wentz, W.H., "Experimental Studies of Flow Separation and Stalling on a Two-Dimensional Airfoil at Low Speeds," NASA CR-2560, 1975.

[4]Wentz, W.H. and Ostowari, C., "Wind Tunnel Studies of Spoiler Flow Characteristics," Dept. of Aeronautical Engineering, AR79-6R, Witchita State Univ., KS, 1979.

[5]Wentz, W.H., Ostowari, C., and Seetharam, H.C., "Effects of Design Variables on Spoiler Control Effectiveness, Hinge Moments and Wake Turbulence," AIAA Paper 81-0072, 1981.

[6]Bodapati, S., Mack, M.D., and Karamcheti, K., "Basic Studies of the Flow Fields of Airfoil-Flap-Spoiler System," AIAA Paper 82-0173, Jan. 1982.

[7]McLachlan, B.G., Karamcheti, K., Ayoub, A., and Hadjidakis, G., "A Study of the Unsteady Flow Field of an Airfoil with Deflected Spoiler," AIAA Paper 83-2131, 1983.

[8]Ayoub, A., Bodapati, S., Karamcheti, K., and Seetharam, H.C., "Unsteady Flow Patterns Associated with Spoiler Control Device," AIAA Paper 82-0127, 1982.

[9]Lee, C.S. and Bodapati, S., "Flow Field Measurements of an Airfoil with Deflected Spoiler," AIAA Paper 83-0365, 1983.

[10]Lee, C.S. and Bodapati, S., "Calculation of the Unsteady Flow Field of an Airfoil with a Deflected Spoiler by Vortex Method," Joint Institute for Aeronautics and Acoustics, TR-62, Stanford Univ., CA, 1985.

[11]Lee, C.S. and Bodapati, S., "An Experimental Study of an Airfoil-Spoiler System," Joint Institute for Aeronautics and Acoustics, TR-61, Stanford Univ., CA, 1985.

[12]Fage, A. and Johansen, F.C., "On the Flow of Air Behind an Inclined Flat Plate of Infinite Span," *Proceedings of Royal Society*, Vol. 116, No. 773, 1927.

[13]Schlichting, H., *Boundary Layer Theory*, Sixth ed., McGraw-Hill, New York, 1968.

[14]Maskew, B. and Dvorak, F.A., "The Prediction of $C_{l\,max}$ Using a Separated Flow Model," *Journal of the American Helicopter Society*, April 1978, pp. 2–8.

[15]Pope, A. and Harper, J.J., *Low-Speed Wind Tunnel Testing*, Wiley, New York, 1965.

[16]Spence, D.A., "Growth of the Turbulent Wake Close Behind an Airfoil at Incidence," Aeronautical Research Council, CP-125, 1953.